Damage propagation at the interface's localization-delocalization transition of the confined Ising model

M. Leticia Rubio Puzzo and Ezequiel V. Albano
Instituto de Investigaciones Fisicoquímicas Teóricas y Aplicadas (INIFTA), UNLP, CONICET, Casilla de Correo 16, Sucursal 4, (1900) La Plata, Argentina

(Received 20 March 2002; revised manuscript received 5 July 2002; published 10 September 2002)

The propagation of damage in a confined magnetic Ising film, with short-range competing magnetic fields (h) acting at opposite walls, is studied by means of Monte Carlo simulations. Due to the presence of the fields, the film undergoes a wetting transition at a well-defined critical temperature $T_w(h)$. In fact, the competing fields cause the occurrence of an interface between magnetic domains of different orientations. For $T<T_w(h)$ $[T>T_w(h)]$ such an interface is bound (unbound) to the walls, while right at $T_w(h)$ the interface is essentially located at the center of the film. It is found that the spatiotemporal spreading of the damage becomes considerably enhanced by the presence of the interface, which acts as a ''catalyst'' of the damage causing an enhancement of the total damaged area. The critical points for damage spreading are evaluated by extrapolation to the thermodynamic limit using a finite-size scaling approach. Furthermore, the wetting transition effectively shifts the location of the damage spreading critical points, as compared with the well-known critical temperature of the order-disorder transition characteristic of the Ising model. Such critical points are found to be placed within the nonwet phase.

DOI: 10.1103/PhysRevB.66.104409 PACS number(s): 75.70.−i, 75.30.Kz, 75.10.Hk, 05.10.Ln

I. INTRODUCTION

The study of the thermodynamic properties of confined systems has attracted considerable attention over the last decades.[1–26] The critical behavior of confined fluids is rather different from the bulk criticality due to the subtle interplay between finite-size and surface effects. The interaction of a saturated gas in contact with a wall or a substrate may result in the occurrence of very interesting wetting and capillary condensation phenomena, where a macroscopically thick liquid layer condenses at the wall, while the bulk fluid may remain in the gas phase.[27–31] The wetting of solid surfaces by a fluid is a phenomenon of primary importance in many fields of practical technological applications (lubrication, efficiency of detergents, oil recovery in porous material, stability of paint coatings, interaction of macromolecules with interfaces, etc.[27,32–34]).

Wetting transitions are also observed when a magnetic material is confined between parallel walls where competing surface magnetic fields act. For example, when an Ising[35,36] film is confined between two competing walls a distance L apart from each other, so that the surface magnetic fields (H) are of the same magnitude but opposite direction, it is found that the competing fields cause the emergence of an interface that undergoes a localization-delocalization transition. This transition shows up at an L-dependent temperature $T_w(L,H)$ that is the precursor of the true wetting transition temperature $T_w(H)$ of the infinite system.[3,10,6,37] It should also be remarked that, although the discussion is presented here in terms of a magnetic language, the relevant physical concepts can rather straightforwardly be extended to other systems such as fluids, polymers, and binary mixtures.

On the other hand, the study and understanding of the propagation of perturbations in magnetic material is also a subject of increasing interest. For this purpose, the damage spreading method is a powerful and useful technique that has been applied, for example, to Ising systems[38–47] as well as to spin glasses,[48,49] for a review see, e.g., Ref. 50.

In order to apply the damage spreading method one has to start from an equilibrium configuration of the magnetic material at temperature T. Such a configuration is generically called the reference or unperturbed configuration $S^A(T)$. Subsequently, a perturbed configuration $S^B(T)$ is obtained just introducing a small perturbation into $S^A(T)$. This procedure can be achieved, e.g., by flipping a small number of spins of the unperturbed configuration. The time evolution of the perturbation is of primary interest because either it can become healed after some time (eventually it may remain finite) or it can propagate over the whole system. The latter scenario may be undesired when a thermally stable magnetic material needs to be achieved. A simple measure of the perturbation is the ''Hamming distance'' or damage between the unperturbed and the perturbed configurations.[38,39] Then the time evolution of the perturbation can be followed evaluating the total damage $D(t)$ defined as the fraction of spins with different orientations, that is,

$$D(t)=\frac{1}{2N}\sum_{l}^{N}|S_l^A(t,T)-S_l^B(t,T)|, \tag{1}$$

where the summation runs over the total number of spins N, and the index l $(1\leqslant l\leqslant N)$ is the label that identifies the spins of the configurations.

In our previous study of damage spreading using Ising magnets confined in two-dimensional geometries[46] and in the absence of external magnetic fields, it has been shown that the presence of interfaces between magnetic domains, in the direction *perpendicular* to the propagation of the damage, causes the spatiotemporal enhancement of the spreading. Due to this interesting feature and in order to contribute to the understanding of the role played by the interfaces, the

aim of this work is to investigate the propagation of the damage at the interface generated by the localization-delocalization transition of the Ising magnet confined in the presence of competing magnetic fields. In this case, and in contrast to the previous work,[46] the propagation of the damage occurs in the direction *parallel* to the interface. In order to carry out the study, Monte Carlo simulations of the Ising magnet in confined, thin-film, geometries are performed. Imposing open boundary conditions and surface magnetic fields along the surfaces of the films, the propagation of the damage in both directions, parallel and perpendicular, to the domain interfaces can be studied. Furthermore, extrapolations of the results to the thermodynamic limit allow us to determine the critical points of damage spreading and locate them in the wetting phase diagram, as evaluated exactly by Abraham.[37]

The manuscript is organized as follows: in Sec. II the numerical procedure for the simulation of damage spreading in confined geometries is described. Section III is devoted to a brief discussion of the equilibrium configurations characteristic of confined geometries with competing applied magnetic fields. The results are presented and discussed the results in Sec. IV, while the conclusions are stated in Sec. V.

II. THE CONFINED ISING FERROMAGNET WITH COMPETING FIELDS AND THE MONTE CARLO SIMULATION METHOD

The Ising model with competing surface fields in a confined geometry of size $L \times M$ ($L \ll M$) can be described by the following Hamiltonian H:

$$H = -J \sum_{\langle ij,mn \rangle}^{M,L} \sigma_{ij}\sigma_{mn} - h_1 \sum_{i=1}^{M} \sigma_{i1} - h_L \sum_{i=1}^{M} \sigma_{iL}, \qquad (2)$$

where σ_{ij} are the Ising spin variables, corresponding to the site of coordinates (i,j), that may assume two different values, namely, $\sigma_{ij} = \pm 1$; $J > 0$ is the coupling constant of the ferromagnet, and the first summation of Eq. (2) runs over all the nearest-neighbor pairs of spins such as $1 \leqslant i \leqslant M$ and $1 \leqslant j \leqslant L$. The second (third) summation corresponds to the interaction of the spins placed at the surface layer $j = 1$ ($j = L$) of the film where a short-range surface magnetic field h_1 (h_L) acts. Open boundary conditions are assumed along the M direction of the film where the fields act.

In this paper, only the case of competing surface fields such as $h_1 = -h_L$, in the absence of any bulk magnetic field, is considered. So, hereafter $h = |h_1| = |h_L|$ will be used generically to specify the short-range surface magnetic field that is measured in units of the coupling constant J. Under these conditions and for a suitable range of fields and temperatures, one may observe the onset of an interface between magnetic domains of opposite direction running along the film, as will be discussed in detail below.

The evolution of the Ising film is simulated using the Glauber dynamics, so a randomly selected spin is flipped with probability $p(flip)$ given by

$$p(flip) = \frac{\exp(-\beta \cdot \triangle H)}{1 + \exp(-\beta \cdot \triangle H)}, \qquad (3)$$

where $\triangle H$ is the difference between the energy of the would-be new configuration and the old configuration, and $\beta = 1/k_B T$ is the usual Boltzmann factor.

The time is measured in Monte Carlo time steps (MCS), such as during one Monte Carlo step all $L \times M$ spins of the sample are flipped once, on the average. The Ising magnet in two dimensions and in the absence of any external magnetic field undergoes a second-order order-disorder transition when the temperature is raised from a relatively low initial value. The critical point is the so called Onsager critical temperature $k_B T_C / J = 2.269 \ldots$.[36]

In order to evaluate the damage according to Eq. (1), first the reference configuration S^A is generated, using the simulation method described above. This can be achieved starting from a random configuration and applying the Glauber dynamics during 10^4 MCS. Subsequently, a replica of such a configuration is created and the spins of the central column ($i = M/2$) are flipped as follows: if the magnetization of the whole sample is greater than zero the up spins are flipped down, otherwise the down spins of the column are flipped up. Using this procedure the perturbed configuration S^B of Eq. (1) is generated and it is assured that the initial damage (at $t = 0$) is always $D(t=0) \leqslant 1/M$. This kind of perturbation reproduces the effect of a large magnetic field applied at the middle of the sample and pointing away to the direction opposite of the actual magnetization of the whole sample.

The time evolution of the damage $D(t)$, evaluated using Eq. (1), is then followed applying the Glauber dynamics to both configurations. At this stage it is essential to use the same random numbers in both systems in order to perform the updates.[50]

Applying the Glauber dynamics to the Ising ferromagnet, it is known that a critical temperature exists for damage spreading (T_D), such as for $T > T_D$ the damage spreads out over the whole sample while for $T < T_D$ the damage becomes healed after some finite time.[50] Extensive numerical simulations done by Grassberger[51,52] have shown that, in two dimensions and in the absence of external magnetic fields, $T_D \cong 0.992 T_C$.

III. DISCUSSION OF EQUILIBRIUM CONFIGURATIONS IN CONFINED GEOMETRIES WITH COMPETING FIELDS

Since the aim of this manuscript is to investigate the role played by the interface between magnetic domains in the propagation of damage, worth discussing are the different equilibrium configurations characteristic of confined geometries under different surface field conditions, close to the wetting phase transition. The situation originated by the presence of competing surface magnetic fields $h_1 = -h_L$ [see Eq. (2)] can be described in terms of a wetting transition that takes place at a certain field-dependent critical wetting temperature $T_w(h)$.[3,9] In fact, for $T < T_w$ a small number of rows parallel to one surface of the film have an overall magnetization pointing to the same direction as the adjacent surface

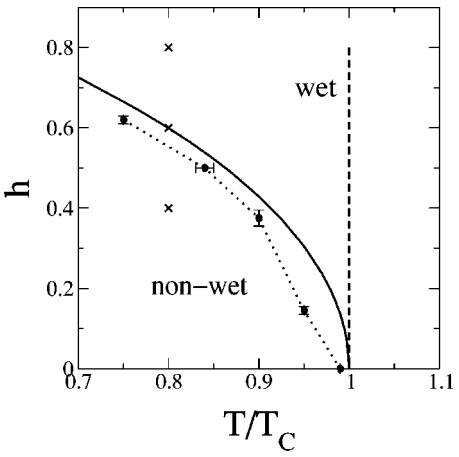

FIG. 1. Wetting phase diagram (h vs T/T_C) corresponding to a semi-infinite Ising strip with opposite short range surface fields. The solid curve is the exact critical line, as obtained by Abraham (Ref. 37). The vertical dashed line is the boundary between the disordered phase at the right-hand side and the ordered one at the left-hand side. The results obtained for the damage spreading transition extrapolated at the thermodynamic limit are shown as filled circles, and the dotted line has been drawn to guide the eyes. Crosses indicate the three points, of the phase diagram, where the snapshots pictures shown in Fig. 2 were obtained.

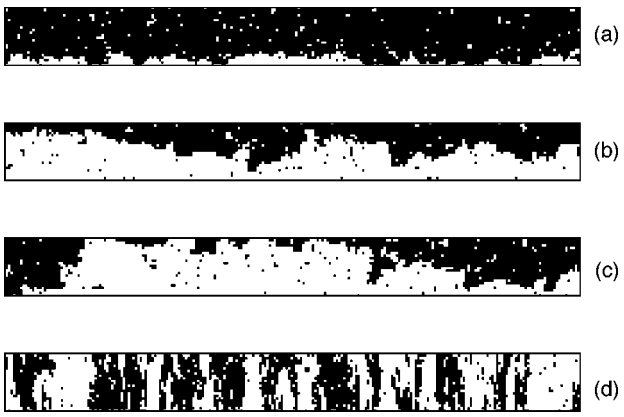

FIG. 2. Snapshot configurations obtained after 10^4 MCS in confined geometries of size $L=24$ and $M=1200$. (a)–(c) Typical spin configurations when short-range fields with opposite signs are applied at bottom and top files of the lattice, respectively. In these cases, the snapshots are taken at $T=0.80T_C$ and different surface fields: (a) $h=0.4$, within the nonwet phase; (b) $h=0.6$, near the critical wetting curve; and (c) $h=0.8$, within the wet phase. The location of these points are shown in the phase diagram of Fig. 1. (d) Typical equilibirum configuration obtained in absence of magnetic fields, applying open boundary conditions, and close to T_C, $T=0.99T_C$. Note that the horizontal coordinate has been reduced by a factor of 5 in comparison with the vertical one for the sake of clarity of the picture. Sites taken by downs spins are shown in black while up spins are left white.

field. However, the bulk of the film has the opposite magnetization (i.e., pointing in the direction of another competing field). Also the symmetric situation is equivalent to the previous one due to the spin-reversal field-reversal symmetry. These configurations, where the interface between domains is tightly bound on the surface, are characteristic of the nonwet phase of the system that occurs at low enough temperatures and fields (see Fig. 1). Increasing the temperature, such an interface moves farther and farther away from the surface towards the bulk of the film. Just at T_w the interface is located in the middle of the film and the system reaches the wet phase for the first time. For $T>T_w$ the interface is no longer localized and the system is within the wet phase (see Fig. 1). For additional details and discussions see, e.g., Ref. 3 and 9.

It should be noticed that the above-discussed wetting transition takes place in the thermodynamic limit only and the phase diagram has been evaluated exactly by Abraham,[37] yielding

$$\exp(2J\beta)\cdot[\cosh(2J\beta)-\cosh(2h_c\beta)]=\sinh(2J\beta), \quad (4)$$

where $h_c(T)$ is the critical surface field [the inverse function of the wetting temperature $T_w(h)$].

As discussed above, a well-defined wetting transition takes place in the thermodynamic limit only. Nevertheless, as shown in Fig. 2 a precursor of this wetting transition can also be observed in confined geometries for finite values of L.[3] This precursor is most correctly described in terms of a localization-delocalization transition of the interface, which takes place at L-dependent critical temperatures [$T_w(L,h)$]. In fact, for $T<T_w(L,h)$ Fig. 2(a)] one observes coexistence of two phases, each of them having opposite magnetization. Furthermore, the interface between domains is located close to one of the surfaces of the film (localized interface; nonwet regime). For $T>T_w(L,h)$ [Fig. 2(c)], the wall between domains moves along the L-direction and the system enters to the wet regime (delocalized interface). The mean position of the interface remains close to the center of the film just at $T_w(L,h)$ [Fig. 2(b)].

According to the finite-size scaling theory[3,6] $T_w(L,h)$ shifts towards $T_w(h)$ according to

$$T_w(\infty,h)-T_w(L,h)\sim \text{const}\times L^{-1}, \quad (5)$$

when the system size L tends to the thermodynamic limit. For further discussions on the localization-delocalization transition of the Ising system in confined geometries see, e.g., Ref. 3 and 10.

Finally, it is worth discussing the equilibrium configurations obtained in the absence of magnetic fields and close below T_C, as shown in Fig. 2(d). In this case the confined system forms a nonuniform state given by a succession of up-spin and down-spin domains, which are essentially ordered at length scales such as the standard correlation length (ξ) remains smaller than the characteristic size of the system ($\xi<L$), but the domain walls are randomly placed. The operation of surface magnetic fields favors the parallel spins, and thus suppresses this domain formation. These facts can be recognized from a visual inspection of the domain patterns shown in Fig. 2.

IV. RESULTS AND DISCUSSION

Monte Carlo simulations have been performed using $L\times M$ lattices, for the choices $L=12$, 24, and 48 and $M=50$

$\times L$. Preliminary runs indicate that the damage spreading transition can be observed, in principle, for any range of temperatures and fields close to the critical wetting line as defined by Eq. (4). However, when the temperature is very low the system becomes almost frozen making difficult the acquisition of data with reliable statistics. Also, for $T>T_C$ the system is disordered preventing the occurrence of the wetting transition. Taking into account these constraints, an extensive study of damage spreading has been performed only close to two particular points of the whole wet nonwet phase diagram, namely, for $|h_1|=|h_L|=0.5$; $T_w(h=0.5) \cong 0.863T_C$, and for $T_w=0.90T_C$; $|h_1|=|h_L|\cong 0.4291$. Additional studies have also been carried out close to $T_w=0.75T_C$; $|h_1|=|h_L|\cong 0.6652$ and $T_w=0.95T_C$; $|h_1|=|h_L| \cong 0.3053$. In view of the obtained results, it is expected that the main conclusions obtained from the study will hold close to the whole critical wetting curve.

In order to characterize the global dynamics of the propagation of the perturbation, the whole damage given by the Hamming distance $D(t)$ [see Eq. (1)] has been evaluated. Also, the survival probability of the damage $P(t)$, that is the probability that at time t the damage is still propagating, has been measured. It should be noted that for a single run, $P(t)$ is a stepped function such as $P(t)=1$ $[P(t)=0]$ if $D(t)>0$ $[D(t)=0]$. The step is located at a certain time, precisely when the damage becomes healed. However, after averaging over a large number of different samples, as in the present work, $P(t)$ becomes a smooth function (see also below).

Also, to study the spatiotemporal evolution of the perturbation, the damage profile in the perpendicular (parallel) $P_x(i,t)$ $[P_y(i,t)]$ direction is defined as follows:

$$P_x(i,t)=\frac{1}{2L}\sum_{j=1}^{L}|S^A_{i,j}(t,T)-S^B_{i,j}(t,T)|, \tag{6}$$

and

$$P_y(j,t)=\frac{1}{2M}\sum_{i=1}^{M}|S^A_{i,j}(t,T)-S^B_{i,j}(t,T)|, \tag{7}$$

where $S^A_{i,j}(t,T)$ and $S^B_{i,j}(t,T)$ are the unperturbed and perturbed equilibrium configurations, respectively. This definition of the perpendicular (parallel) damage profile represents the average damaged sites of the ith–$i=1,\ldots,M$ column (jth–$j=1,\ldots,L$ row) of the lattice. In order to characterize the profiles it is also useful to determine their widths $[\langle\omega_x(t)\rangle$ and $\langle\omega_y(t)\rangle]$, as well as their amplitudes $[\langle h_x(t)\rangle$ and $\langle h_y(t)\rangle]$, respectively. The propagation of the damage is studied using two approaches: (i) keeping $h=0.5$ constant and varying T, and (ii) keeping $T=0.90T_C$ constant and varying h.

A. The case $h=0.5$, T variable

Figure 3 shows log-log plots of the damage $D(t)$ as a function of time. It is interesting to note that the localization-delocalization transition is roughly revealed by the behavior of the damage. In fact, for $T<T_w(L)$ [e.g., for $T=0.70T_C$, $0.65T_C$, and $0.60T_C$ in Fig. 3(a)] it is observed that the damage is healed after a relatively short time. However for $T>T_w(L)$ [e.g., for $T=0.80T_C$ and $0.85T_C$ in Fig. 3(a)] the spreading of damage is actually observed.

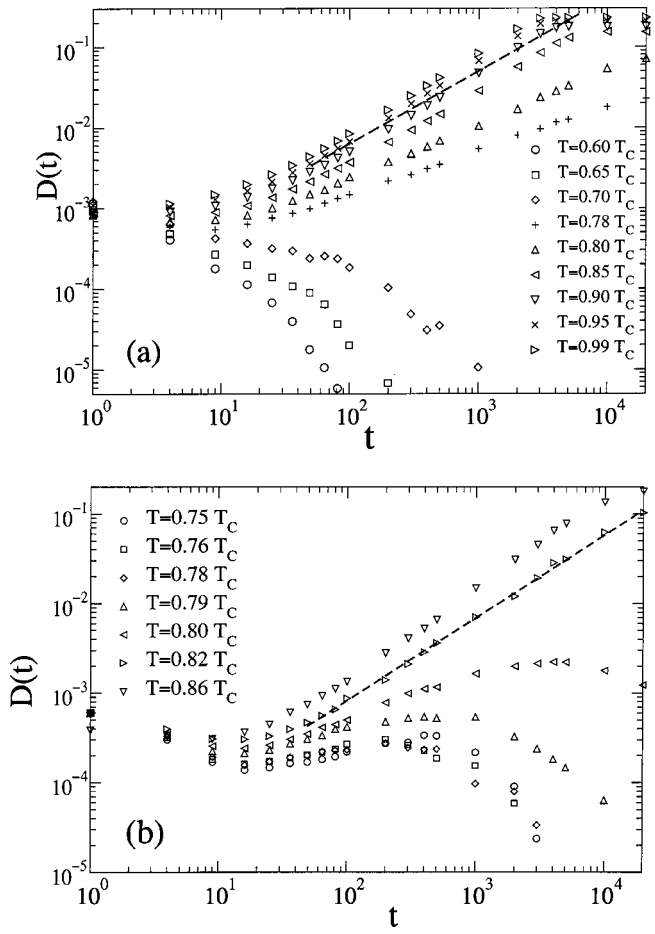

FIG. 3. Log-log plots of $D(t)$ vs t obtained at different temperatures as indicated in the figure, applying short-range fields of magnitude $h=0.5$, and using lattices of sizes (a) $L=12$, $M=601$ and (b) $L=24$, $M=1201$. The dashed lines have slopes $\eta=0.90$ and have been drawn for the sake of comparison.

It should be noticed that using finite lattices, the onset of damage spreading is observed at L-dependent "critical" temperatures $[T_D(L)]$, while the actual damage spreading transition is defined in the thermodynamic limit only, i.e., at $T_D(\infty)$. The latter can be obtained using an extrapolation procedure, similar to that given by Eq. (5), as will be discussed below. As expected, finite-size effects cause the actual transition to become rounded and shifted, as, e.g., can be observed comparing Figs. 3(a) and 3(b), which have been obtained using lattices of different sizes. The straight lines observed in Figs. 3(a) and 3(b) for $T\geqslant T_D(L)$ suggest a power-law behavior such as

$$D(t)\propto t^{\eta}, \tag{8}$$

where η is an exponent. Disregarding the early time behavior of $D(t)$ (say, up to $t\approx 30$ MCS), the best fit of the data shown in Fig. 3(a), using Eq. (8), gives $\eta\cong 0.90\pm 0.02$. Simulations performed using bigger lattices [$L=24$, and 48,

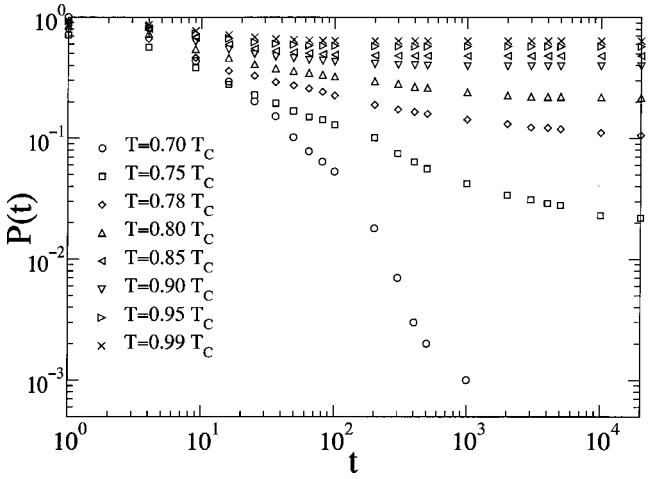

FIG. 4. Log-log plots of $P(t)$ vs t obtained at different temperatures as indicated in the figure, and using lattices of size $L=12$ and $M=601$. Short-range fields of magnitude $h=0.5$ are applied at the walls of the sample.

see, e.g., Fig. 3(b)] also give $\eta \cong 0.91 \pm 0.01$, where in all cases the error bars merely reflect the statistical error.

Notice that damage spreading is also observed for a temperature slightly below T_w [e.g., at $T=0.80T_C$ in Fig. 3(a) and $T=0.82T_C$ in Fig. 3(b)]. This observation is due to the operation of finite-size effects causing the effective location of the prewetting temperature to be slightly below T_w [see Eq. (5)]. Eventually, this result may also indicate that the critical temperature for damage spreading lies below T_w, as will be discussed below.

The survival probability of the damage $P(t)$ is shown in Fig. 4, as a function of time t. It is observed that $P(t)$ tends to vanish for $T<T_D(L)$, while it reaches a stationary value for $T>T_D(L)$. So, it is possible to define the stationary survival probability P_{stat} as the asymptotic limit $P_{stat} \equiv P(t \rightarrow \infty)$ [see Fig. 5(a)]. In this case, finite-size effects are also observed. In fact, the step function expected for the $P_{stat}(T)$ becomes rounded for lattices of sizes $L=12$ and $M=601$. However, the damage temperature $T_D(L)$ can be determined as the mean value of the rounded step.

Figure 6 shows log-log plots of the width of the damage profile $\langle \omega_x(t) \rangle$ vs t obtained taking $h=0.5$ and different temperatures. It is observed that for $T>T_D(L)$ $[T<T_D(L)]$ the width exhibits an upward (downward) curvature. However, straight-line behavior emerges for a certain temperature that is identified as $T_D(L) \approx 0.78$. Based on these observations, the following scaling law is proposed,

$$\langle \omega_x(t) \rangle \propto t^{\alpha}, \tag{9}$$

where α is an exponent. The best fit of the data gives $\alpha = 0.80 \pm 0.01$.

It is worth mentioning that different behavior has been observed for zero surface fields $(h=0)$ close to the critical temperature.[46] In this limit the critical temperature for damage spreading is well known, namely, $T_D(h=0, L=\infty) \simeq 0.992T_C$.[51,52] However, in this case a crossover between a short-time regime and a long-time regime is found close to

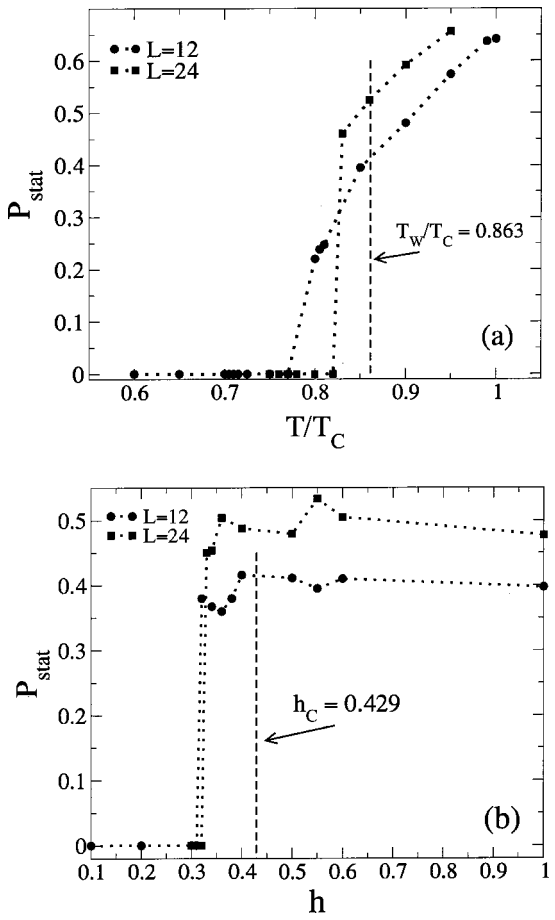

FIG. 5. Plots of the stationary survival probability $P_{stat} \equiv P(\rightarrow \infty)$ as obtained using lattices of sizes $L=12$ $(M=601)$, and $L=24$ $(M=1201)$. (a) P_{stat} vs T/T_C obtained taking short-range fields of magnitude $h=0.5$ (the dotted lines have been drawn to guide the eyes). The vertical dashed line indicates the exact critical wetting point: $T_w(h_C=0.5)=0.863T_C$. (b) P_{stat} vs h obtained taking a fixed temperature $T=0.90T_C$ (the dotted lines have been drawn to guide the eyes). The vertical dashed line corresponds to the exact wetting critical point: $h_C(T_w=0.90T_C)=0.4291$.

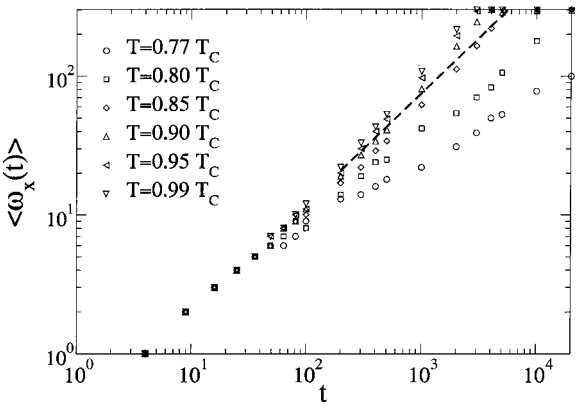

FIG. 6. Log-log plots of $\langle \omega_x(t) \rangle$ vs t obtained at different temperatures, as indicated in the figure, using lattices of size $L=12$, $M=601$, obtained taking short-range fields of magnitude $h=0.5$. The dashed line has a slope $\alpha=0.80$.

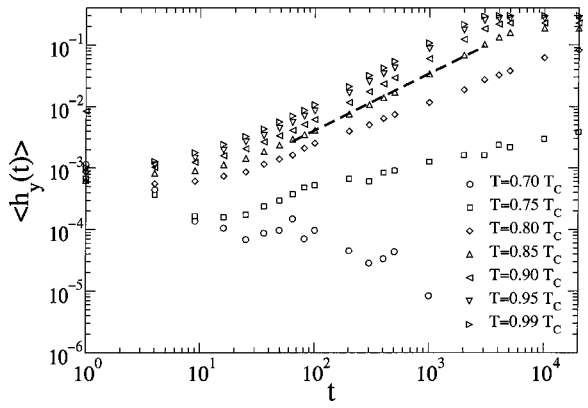

FIG. 7. Log-log plots of $\langle h_y(t)\rangle$ vs t obtained at different temperatures, as indicated in the figure, using lattices of size $L=12$, $M=601$, and applying short-range fields of magnitude $h=0.5$. The dashed line has a slope $\lambda=0.98$.

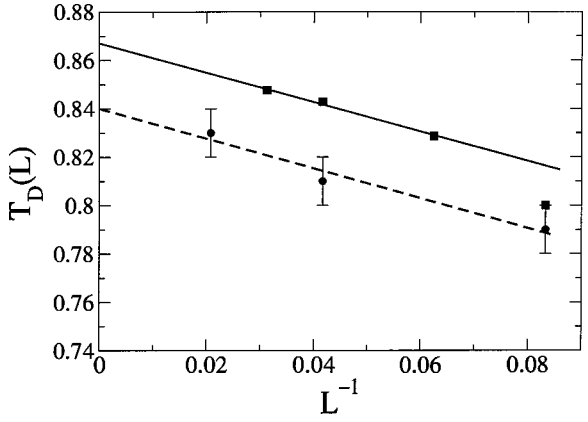

FIG. 8. Damage spreading critical points $T_D(L)$ as a function of L^{-1}, obtained for lattices of different sizes ($L=12$, 24, and 48, with $M=50\times L$), and applying short-range surface fields of magnitude $h=0.5$ (filled circles). The dashed line extrapolates to the critical temperature $T_D/T_C=0.84\pm0.01$. Filled squares correspond to the interface localization-delocalization transitions $T_w(L)$ as obtained for $h=0.5$ and using the criteria of the maximum of the susceptibility (Ref. 3). The solid line extrapolates to the wetting critical temperature $T_w/T_C=0.863$.

$t\simeq350$ MCS. For $t<350$ MCS the data is consistent with $\alpha_{ST}=0.517\pm0.005$, while for $t>350$ MCS one has $\alpha_{LT}=0.79\pm0.01$. These results also suggest that diffusivelike behavior, as expected for $\alpha=1/2$, dominates the short-time regime, while the propagation of the perturbation becomes faster within the long-time regime.[46]

The observed difference between the cases $h>0$ and $h=0$ can be understood with the aid of the snapshot configurations shown in Figs. 2(a)–2(c) and 2(d), respectively. In fact, when the interface is most likely localized at the center of the strip running parallel to the M direction, where the surface magnetic fields are applied, one expects a uniform propagation of the perturbation as observed in Fig. 6. However, for $h=0$ the occurrence of magnetic domains of opposite orientation exhibiting interfaces running perpendicular to the strip determines the onset of two different time regimes: on the one hand the short-time regime, characterized by the (slow) propagation of the damage inside the bulk of magnetic domains and, on the other hand, the long-time regime with a (faster) propagation of the perturbation effectively catalyzed by large fluctuations occurring at the interfaces of the domains.

The amplitude of the damage profile in the direction parallel to the interface $\langle h_y(t)\rangle$, as shown in Fig. 7, also exhibits its power-law behavior of the type

$$\langle h_y(t)\rangle \propto t^{\lambda}, \tag{10}$$

where λ is an exponent. A least-squares fit of the data (see Fig. 7) gives $\lambda=0.98\pm0.01$, for $T\geqslant T_D(L)$. Also, the damage tends to become healed for $T<T_D(L)$. Simulations performed using bigger lattices shows that this exponent tends to $\lambda\approx1$ for the asymptotic limit, $L\to\infty$, e.g., $\lambda(L=24)=1.03\pm0.02$ and $\lambda(L=48)=1.04\pm0.05$.

It is interesting to remark on the behavior of the damage profiles along the direction parallel to the applied fields, close to $T_D(L)$.[47] In the absence of surface fields and using open boundary conditions, the homogeneous propagation of the damage is observed. However, considering competing surface fields the damage is greater in the region where the interface between magnetic domains is located, namely, at the central rows of the film ($i\sim L/2$). This fact is in qualitative agreement with the results discussed for $\langle h_y(t)\rangle$. These observations are consistent with the fact that large fluctuations capable of catalyzing the propagation of the damage are present along the interface, while at the walls and due to the applied magnetic fields, the orientation of the spins is more stable. It should be noted that due to the finite size of the lattice, the width of the damage profile $\langle \omega_y(t)\rangle$, remains constant close to $L/2$, preventing a quantitative analysis.

Based on the study of $D(t)$, $P(t)$, and the damage profiles, the location of the L-dependent damage spreading critical points $T_D(L)$, for a fixed field $h=0.5$, have been estimated as follows: $T_D(L=12)=0.79(1)T_C$, $T_D(L=24)=0.81(1)T_C$, and $T_D(L=48)=0.83(1)T_C$. Based on these results and assuming that $T_D(L)$ obeys a scaling law such as Eq. (5), the extrapolation $T_D(\infty)=0.84\pm0.01$ has been obtained, as shown in Fig. 8. This value is close to (but smaller than) the wetting critical temperature $T_w(h=0.5)=0.863$, as evaluated using Eq. (4) (see also Fig. 1). It is known that one method to locate the L-dependent critical temperatures for the localization-delocalization transition $[T_w(L)]$, which is the precursor of the true wetting temperature in the thermodynamic limit, is the evaluation of the maximum of the susceptibility, i.e., the fluctuations of the order parameter.[3] Figure 8 also shows that a plot of $T_w(L)$ vs L^{-1} [see Eq. (5)] extrapolates to $T_w(L\to\infty)=0.863$, in good agreement with the exact value. Furthermore, one has that $T_D(L)<T_w(L)$. At this stage it is concluded that, on the one hand, it is hard to establish an unambiguous difference between T_D and T_w, while on the other hand, it is no doubt that the onset of damage propagation is related to the localization-delocalization transition that undergoes the interface between competing domains, so that T_D is effectively shifted to temperatures far below T_C.

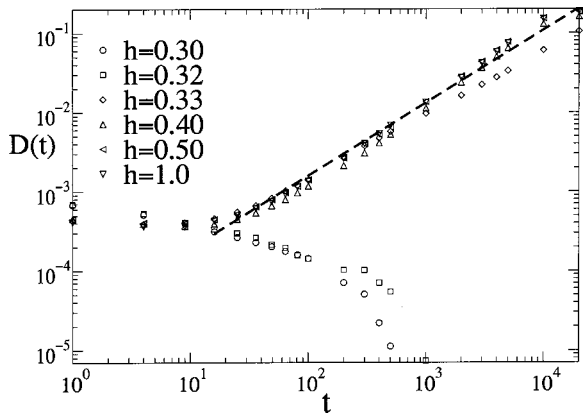

FIG. 9. Log-log plots of $D(t)$ vs t obtained using short-range magnetic fields of different magnitude as indicated in the figure, at fixed temperature $T=0.90T_C$, and using lattices of size $L=24$, $M=1201$. The dashed line has a slope $\eta\sim0.90$.

B. The case $T=0.9T_C$, h variable

In this case, the obtained results are fully consistent with those obtained keeping the field constant and varying the temperature. In fact, the total damage $D(t)$ grows up for $h>h_D(L)$ with exponent $\eta=0.91\pm0.02$ (see Fig. 9), where $h_D(L)$ is the L-dependent "critical" field for damage spreading. In fact, as in the case treated in the previous subsection, the actual critical field $h_D(\infty)$ is defined in the thermodynamic limit only. As in the previous cases, it is observed that for lattices of size $L=12$, the damage spreading transition is markedly rounded by finite-size effects, while for $L=24$ or $L=48$ that transition is better defined.

The stationary survival probability of the damage P_{stat} can also be determined, as shown in Fig. 5(b), as a function of the surface field h. The fact that the stepped shape of P_{stat} is better defined in Fig. 5(b) than in Fig. 5(a) is an intriguing feature that remains to be clarified. The width of the damage profile also behaves according to a power law [see Eq. (8)] with an exponent $\alpha=0.81\pm0.01$ (see Fig. 10), in full agreement with our previous estimation given by $\alpha=0.80\pm0.01$.

It is found that the amplitude of the profile, $\langle h_y(t)\rangle$, also exhibits a power law close to T_D (Fig. 11). In fact, the exponent λ [see Eq. (10)] has been determined given $\lambda=1.02\pm0.01$, in full agreement with our estimation obtained keeping constant the surface fields, namely, $\lambda=0.98\pm0.01$.

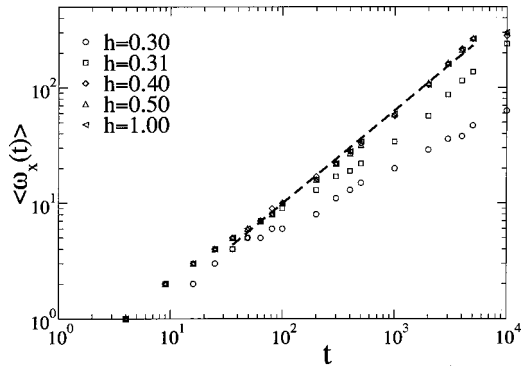

FIG. 10. Log-log plots of $\langle\omega_x(t)\rangle$ vs t obtained for short-range magnetic fields of different magnitude, as indicated in the figure, using lattices of size $L=12$, $M=601$, and at fixed temperature $T=0.90T_C$. The dashed line has slope $\alpha=0.81$.

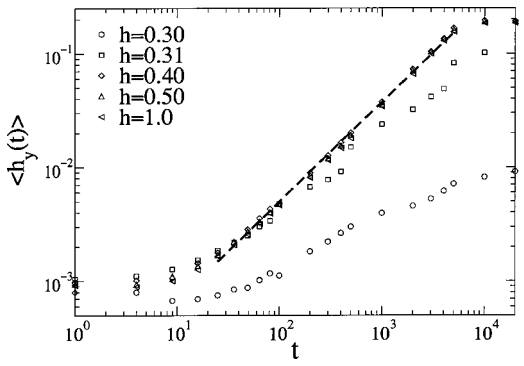

FIG. 11. Log-log plots of $\langle h_y(t)\rangle$ vs t obtained at different short-range magnetic fields, as indicated in the figure, using lattices of size $L=12$, $M=601$, and at fixed temperature $T=0.90T_C$. The dashed line has a slope $\lambda=1.02$.

It has been observed that the amplitude along the parallel direction and the width of the profiles across the perpendicular direction [$\langle h_x(t)\rangle$ and $\langle\omega_y(t)\rangle$, respectively] exhibit the same behavior as in the previous case with constant surface fields, so the corresponding figures are omitted for the sake of space. Finally, our estimations of the size-dependent damage spreading critical fields $h_D(L)$ are given by $h_D(L=12)=0.31(2)$, $h_D(L=24)=0.34(1)$, and $h_D(L=48)=0.35(1)$.

By comparison to Eq. (5) the following finite-size scaling anzatz can be expected to hold for the wetting critical field:

$$h_c(L)-h_c(\infty)\sim\text{const}\times L^{-1}, \tag{11}$$

where $h_c(\infty)$ is the position of the critical point in the thermodynamic limit. Plotting the obtained data for the damage spreading critical fields according to Eq. (11) (Fig. 12), the extrapolation to $L\to\infty$ gives $h_D(L=\infty)=0.37\pm0.02$, while the exact value for the wetting critical point at $T=0.9T_c$, as obtained using Eq. (4), is $h_c=0.429\,06$. As in the previous

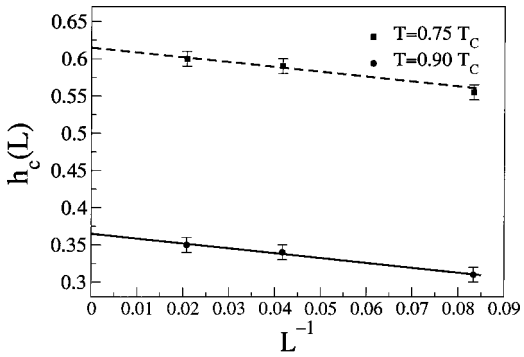

FIG. 12. Damage spreading critical fields $h_D(L)$ as a function of L^{-1}, obtained for lattices of different sizes ($L=12$, 24, 48), and at different temperatures, as indicated in the figure. The dashed (solid) line extrapolates to the critical field $h_D(L\to\infty,T=0.75T_C)=0.62\pm0.01$ [$h_D(L\to\infty,T=0.90T_C)=0.37\pm0.02$]. Both lines have the same slope.

case, the location of the damage spreading critical point lies slightly inside the nonwet region of the phase diagram (see Fig. 1).

C. Complementary studies

In order to confirm the findings of the previous sections, additional simulations were performed at $T=0.75T_C$ and $T=0.95T_C$ and varying the surface fields. All the obtained results are consistent with the previous findings. In summary, applying the scaling anzatz given by Eq. (11), the critical field for damage spreading $h_D(\infty)=0.62\pm0.01$ $[h_D(\infty)=0.15\pm0.01]$ was obtained, as compared with the exact result for the wetting critical point [e.g., Eq. (4)] given by $h_c(T=0.75T_C)=0.6652$ $[h_c(T=0.95T_C)=0.3053]$. Notice that the former extrapolation is shown in Fig. 12.

All results reported previously have so far been obtained using lattices of aspect ratio $L/M=50$. Additional runs were also performed taking $L/M=2$, 10, and 25. Results obtained using $L/M=2$ are strongly hindered by finite-size effects since, above the effective damage critical point, the damage quickly reaches the boundary of the sample. Increasing the aspect ratio the results are in agreement with those obtained using $L/M=50$. So, it is expected that the main conclusions obtained in this work should be independent of the aspect ratio of the samples, provided that large values of this parameter are used.

V. CONCLUSIONS

Based on an extensive numerical study of the damage propagation close to the wetting transition of the Ising model with competing fields it is possible to draw the following main conclusions:

(i) The exponent governing the spreading of the total damage $[D(t)\propto t^{\eta}$, see Eq. (8)], in the presence of interfaces in the direction parallel to the propagation of the perturbation, namely, $\eta\cong0.90\pm0.02$, is greater than those obtained in the absence of the interface, namely, $\eta\cong0.471\pm0.005$.[41,46] So, clearly the interface causes the enhancement of the propagation of the perturbation.

From a more qualitative point of view, it is expected that the propagation of damage may be favored by interfaces because precisely around these regions of the sample one has the largest fluctuations in the orientation of the spins. Within this scenario the spreading of the damage is expected to be faster along the direction parallel to the interface where the fluctuations can uniformly be propagated. In contrast, the spreading along the direction perpendicular to the interface may be slowed down by the periods where the damage has to cross over the bulk of the domains.[46]

(ii) Clear evidence on the shift of the critical damage temperature is reported. In fact, while it is well known that $T_D(h=0)\approx0.992T_C$ in the absence of surface magnetic fields,[51,52] our findings show that $T_D(h>0)<T_D(h=0)$ when competing surface fields are applied. Furthermore, all the damage spreading critical points extrapolated to the thermodynamic limit lie systematically within the nonwet phase of the wetting phase diagram (Fig. 1). These results suggest that the wetting and the damage spreading critical curves are different and point out that the former should be slightly shifted towards the nonwet phase. We expect that the shift of the critical damage temperature due to the presence of competing surface fields is a fundamental property of the damage in the Ising magnet which may be independent of the adopted dynamics. In contrast, the location of the critical damage spreading points within the nonwet phase may be a property only related to the employed dynamics (Glauber, in the present work). Regrettably, the clarification of these points remains open and deserves further studies, including the use of different dynamics such as Metropolis, heat-bath, etc.[53]

We expect that this numerical work may contribute to the understanding of the role of interfaces in the propagation of damage. The overall understanding of these complex physical phenomena addresses a significant theoretical and experimental challenge. Such kinds of studies are stimulated by many practical and technological applications such as, e.g., the design and construction of high-quality magnetic materials.

ACKNOWLEDGMENTS

This work was supported financially by CONICET, UNLP, and ANPCyT (Argentina). M.L.R.P. acknowledges the National Academy of Exact Sciences (Argentina) for financial support.

[1] M. E. Fisher and H. Nakanishi, J. Chem. Phys. **75**, 5857 (1981).
[2] H. Nakanishi and M. E. Fisher, J. Chem. Phys. **78**, 3279 (1983).
[3] E. V. Albano, K. Binder, D. Heermann, and W. Paul, Surf. Sci. **223**, 151 (1989).
[4] E. V. Albano, K. Binder, D. Heermann, and W. Paul, J. Stat. Phys. **61**, 161 (1990).
[5] A. O. Parry and R. Evans, Phys. Rev. Lett. **64**, 439 (1990).
[6] M. R. Swift, A. L. Owczarek, and J. O. Indekeu, Europhys. Lett. **14**, 465 (1991).
[7] U. Gradmann, J. Magn. Magn. Mater. **100**, 481 (1991).
[8] K. Binder and D. P. Landau, J. Chem. Phys. **96**, 1444 (1992).
[9] A. O. Parry and R. Evans, Physica A **181**, 250 (1992).
[10] K. Binder, D. P. Landau, and A. M. Ferrenberg, Phys. Rev. Lett. **74**, 298 (1995); Phys. Rev. E **51**, 2823 (1995).
[11] K. Binder, D. P. Landau, and A. M. Ferrenberg, Phys. Rev. E **53**, 5023 (1995).
[12] A. Maciolek and J. Stecki, Phys. Rev. B **54**, 1128 (1996).
[13] A. Maciolek, J. Phys. A **29**, 3837 (1996).
[14] A. Wener, F. Schmid, M. Mueller, and K. Binder, J. Chem. Phys. **107**, 8175 (1997).
[15] D. Karevski and M. Henkel, Phys. Rev. B **55**, 6429 (1997).
[16] E. Carlon and A. Drzewiński, Phys. Rev. E **57**, 2626 (1998).
[17] E. Carlon, A. Drzewiński, and J. Rogiers, Phys. Rev. B **58**, 5070 (1998).
[18] A. M. Ferrenberg, D. P. Landau, and K. Binder, Phys. Rev. E **58**, 3353 (1998).

[19] H. Liu, A. Bhattacharya, and A. Chakrabarti, J. Chem. Phys. **109**, 8607 (1998).
[20] T. Aign, P. Meyer, S. Lemerle, J. P. Jamet, J. Ferre, V. Mathet, C. Chappert, J. Gierak, C. Vieu, F. Rousseaux, H. Launois, and H. Bernas, Phys. Rev. Lett. **81**, 5656 (1998).
[21] H. L. Frisch, S. Puri, and P. Niebala, J. Chem. Phys. **110**, 10 514 (1999).
[22] J. Slen, A. K. Swan, and J. F. Wendelken, Appl. Phys. Lett. **75**, 2987 (1999).
[23] J-S. Tsay and Y-D. Yao, Appl. Phys. Lett. **74**, 1311 (1999).
[24] E. V. Albano, K. Binder, and W. Paul, J. Phys.: Condens. Matter **12**, 2701 (2000).
[25] M. Mueller, E. V. Albano, and K. Binder, Phys. Rev. E **62**, 5281 (2000).
[26] F. D. A. Aarão Reis, Phys. Rev. B **62**, 6565 (2000).
[27] P. G. de Gennes, Rev. Mod. Phys. **57**, 827 (1985).
[28] S. Dietrich, in *Phase Transitions and Critical Phenomena*, edited by C. Domb and J. L. Lebowitz (Academic Press, London, 1988), Vol. 12, p. 1.
[29] G. Forgacs, R. Lipowsky, and Th. M. Nieuwenhuizen, in *Phase Transitions and Critical Phenomena*, edited by C. Domb and J. L. Lebowitz (Academic Press, London, 1991), Vol. 14.
[30] A. O. Parry, J. Phys.: Condens. Matter **8**, 10 761 (1996).
[31] D. E. Sullivan and M. M. Telo da Gama, in *Fluid and Interfacial Phenomena*, edited by C. A. Croxton (Wiley, New York, 1986).
[32] F. Iglói and I. O. Indeku, Phys. Rev. B **41**, 6836 (1990).
[33] C. Ebner, F. Hayot, and J. Cai, Phys. Rev. B **42**, 8187 (1990).
[34] Y. Le Bouar, A. Loiseau, A. Final, and F. Ducastelle, Phys. Rev. B **61**, 3317 (2000).
[35] E. Ising, Z. Phys. **31**, 253 (1925).
[36] B. M. McCoy and T. T. Wu, *The Two-dimensional Ising Model* (Harvard University Press, Cambridge, MA, 1973).
[37] D. B. Abraham, Phys. Rev. Lett. **44**, 1165 (1980).
[38] B. Derrida and D. Stauffer, Europhys. Lett. **2**, 739 (1986).
[39] H. E. Stanley, D. Stauffer, J. Kertesz, and H. J. Herrmann, Phys. Rev. Lett. **59**, 2326 (1987).
[40] P. Grassberger, Physica A **214**, 547 (1995).
[41] F. Montani and E. V. Albano, Phys. Lett. A **202**, 256 (1995).
[42] F. Wang, N. Hatano, and M. Suzuki, J. Phys. A **28**, 4543 (1995).
[43] T. Vojta, J. Phys. A **30**, L7 (1997).
[44] A. V. Lima, M. L. Lyra, and U. M. S. Costa, J. Appl. Phys. **81**, 3983 (1997).
[45] A. V. Lima, M. L. Lyra, and U. M. S. Costa, J. Magn. Magn. Mater. **171**, 329 (1997).
[46] E. V. Albano and M. L. Rubio Puzzo, Physica A **293**, 517 (2001).
[47] E. V. Albano and M. L. Rubio Puzzo, J. Magn. Magn. Mater. **241**, 110 (2002).
[48] B. Derrida and G. Weisbuch, Europhys. Lett. **4**, 657 (1987).
[49] C. Argolo, A. M. Mariz, and S. M. Miyazima, Physica A **264**, 142 (1999).
[50] H. J. Herrmann, *Damage Spreading in Computer Simulation Studies in Condensed Matter Physics II*, edited by D. P. Landau, K. K. Mon, and H. -B. Schüttler (Springer, Berlin, 1989), Part I, p. 56.
[51] P. Grassberger, J. Phys. A **28**, L67 (1995).
[52] P. Grassberger, J. Stat. Phys. **79**, 13 (1995).
[53] S. C. Glotzer, P. H. Poole, and N. Jan, J. Stat. Phys. **68**, 895 (1992).